Smart Structures and Systems, *Vol. 27, No. 4 (2021) 667-678*
DOI: https://doi.org/10.12989/sss.2021.27.4.667

Thermal postbuckling of shear deformable multiscale hybrid composite beams

Arameh Eyvazian [1,2], Chunwei Zhang*[1], Mohammad Alkhedher [3], Murat Demiral [4], Afrasyab Khan [5] and Tamer A. Sebaey [6,7]

[1] *Structural Vibration Control Group, Qingdao University of Technology, Qingdao 266033, China*
[2] *Department of Mechanical Engineering, Politecnico di Milano (Technical University), Via La Masa 1, 20156 Milan, Italy*
[3] *Mechanical Engineering Department, Abu Dhabi University, Abu Dhabi 59911, UAE*
[4] *College of Engineering and Technology, American University of the Middle East, Kuwait*
[5] *Institude of Engineering and Technology, Department of Hydraulics and Hydraulic and Pneumatic Systems, South Ural State University, Lenin Prospect 76, Chelyabinsk, 454080, Russian Federation*
[6] *Engineering Management Department, College of Engineering, Prince Sultan University, Riyadh, Saudi Arabia*
[7] *Mechanical Design and Production Department, Faculty of Engineering, Zagazig University, P.O. Box 44519, Zagazig, Sharkia, Egypt*

(*Received June 11, 2020, Revised November 9, 2020, Accepted November 25, 2020*)

Abstract. This research is deal with thermal buckling and post-buckling of carbon nanotube/fiber/polymer composite beams. The beam is considered to be under uniform temperature rise. Firstly, the effective material properties of a two phase nanocomposite consisting of CNT and polymer are extracted. Then, the modified Chamis rule is utilized to obtain the equivalent thermo-mechanical properties of multiscale hybrid composite (MHC). Based on the first order shear deformation theory, Von-Karman type of geometrically nonlinear strain-deformation equations and also the virtual work rule, the equilibrium equations of a three phace composite beam are derived. Bifurcation buckling and also the thermal post-buckling is analysed using the generalized differential quadrature technique. In the thermal buckling phenomena, a linear eigenvalue problem is solved; however, due to the nonlinearity, the thermal postbuckling study is performed using an iterative displacement control strategy. After validation study, several novel results demonstrate the influences of length-to-thickness ratio, agglomeration of applied CNTs and fibers in the composite media and number and orientation of layers on the critical temperature and displacement-loading path.

Keywords: MHC beam; nonlinear thermal stability; GDQM; displacement control strategy

1. Introduction

Composite structures are frequently manufactured and analyzed in the industry and laboratory practise. The first type of composites involves matrix and macro size fibers, while lightweight, has very appropriate thermal and mechanical properties. In the last decades, nano size reinforcements such as carbon nonotubes (CNTs) are more antecedent due to their supernatural thermal, electrical, and mechanical characteristics (Nguyen and Pham 2017, Dat *et al*. 2020a, b, Duc *et al*. 2019a, Van Thanh *et al*. 2019, Han *et al*. 2019). The synthesis of nano reinforcements and matrix is called nanocomposites. In addition, there are many other nanoscale fillers, where the most favorite of them are graphene (Safaei *et al*. 2019, Fattahi *et al*. 2019a, b, Talebizadehsardari *et al*. 2020a), grapheme platelets (GPL) (Eyvazian *et al*. 2020a, b, c) and graphene oxide (GO) (Motezaker and Eyvazian 2020). One of the modern class of composites includes three phases, namely macroscale/ nanoscale reinforcements and matrix. This type of composites is mentioned multiscale hybrid composite (MHC) in the literature. Researches on the MHCs divide into three classifications: 1. Manufacturing 2. Material properties 3. Thermo/Mechanical behaviors.

Among the preliminary works on the fabricating MHCs, Thostenson *et al*. (2002) utilizing the chemical vapor deposition procedure (VDP) created a single-fiber which the carbon nonotubes surround it. This paper has demonstrated that growing the CNT significantly improves the interfacial load transfer in the composite. In another work, Song (2007) constructed a multiscale composite with CNTs/aramid/epoxy phases by means of vacuum-assisted resin transfer modeling (VARTM). A dramatically amelioration is observed in the flexural properties of the foresaid three phase composite. Based on a study by Bekyarova *et al*. (2007a), about 30% enhancement of the interlaminar shear strength is viewed by adding the CNTs in the carbon fiber (CF) composite. Furthermore, remarkable increment of out-of-plane electrical conductivity is illustrated between CNT/CF/epoxy and CF/epoxy. In another work by these authors (Bekyarova *et al*. 2007b), the mechanical tests depicted that implementing the CNTs into the CF/epoxy composite mechanical properties increased sharply. Kim *et al*. (2009) reported 11.6%, 18%, and 11.4% modification in the flexural modulus, strength, and percent strain to break, respectively, by augmenting the carbon nanotubes in the carbon fiber/resin composite. It is worth nothing that in this paper, a high-energy sonication

*Corresponding author, Ph.D.,
E-mail: zhangchunwei@qut.edu.cn

ISSN: 1738-1584 (Print), 1738-1991 (Online)

technique is employed to invent the MHC.

There are various ongoing researches on the material properties of such composites. In this paper, only a few articles that have worked on the thermal and mechanical properties are mentioned. For instance, Sung *et al*. (2018) explored the thermal conductivity of multiscale hybrid composite made of CNT/woven fiber/polymer implementing an effective analytical method. By means of electrophoretic deposition of carboxylic acid- or amine-functionalized carbon nanofibers (CNFs) on the surface of carbon fiber, multiscale reinforcement fabrics are made by Rodriguez *et al*. (2011). They highlighted that the panel with amine-functionalized CNFs had a substantial increase in interlaminar shear strength (ILSS) and compressive strength compared to a base composite. Rahmanian *et al*. (2014) calculated an optimum amount of CNT in the MHCs to obtain the maximum impact resistance, strength, and elastic and storage modulus. In this experiment, the CNTs are grown on fibers using the chemical vapor deposition (CVD) technique. Radue and Odegard (2018) demonstrated an analysis to predict the mechanical characteristics of a three phase composite employing the molecular dynamic simulation (MDS). Furthermore, in this article, the effects of adding CNTs on the several classes of resins are investigated. Rahman *et al*. (2012) determined the optimized mechanical and thermal properties of e-glass/epoxy composite by incorporating the multi-walled CNT in the structure. To diminish the residual stress in the two phase composites, Shokrieh and his co-workers (Shokrieh *et al*. 2013) synthesized the carbon nanofibers and two phase CF/epoxy composite. They proved that enhancement of 1 wt.% carbon nanofibers resulted in 25.1% reductions in residual stress.

Recently, the astonishing effects of the addition of carbon nanotubes on the thermal and mechanical behavior of composite structures have attracted the attention of many scientists. Rafiee *et al*. (2014a) investigated the influence of piezoelectric layers on the nonlinear stress behavior of MHC plates. Halpin-Tsai and fiber micromechanical rules are used to obtain the effective material properties of composite plate. It is depicted that increasing a small CNT magnitudes splendidly decrease the bending deflection. Also, they compare effect of multi-walled and single-walled CNTs on the stresses and deflection and it is demonstrated that the single-walled CNTs has more effect on the reduction of stresses and bending deformations. In another work of this author (Rafiee *et al*. 2018), a cross sectional design study for MHC beams and blades under various mechanical tests are examined. Large amplitude bending probe is analyzed for MHC plate based upon the third order shear deformation theory by Gholami and Ansari (2018). In this paper, generalized differential quadrature and arc-length techniques are used. The effect of incorporation CNTs in the fibrous composite plates and disks on the reduction the residual stress are studied by Ghasemi *et al*. (2015, 2017). Utilizing the GDQ method, frequency characteristics study of non-uniform MHC beams is performed by Seidi and Kamarian (2016). In this manuscript, the impacts of carbon nanotube agglomeration and various lay-ups are also examined. Ebrahimi and Dabbagh (2019) applied Galerkin method to solve mechanical vibration problem for MHC beams in the thermal environment. Geometrically nonlinear vibration of MHC beams with considering the viscosity based on the Caputo fractional derivative model are analyzed by He *et al*. (2015). Nonlinear vibration of MHC plate embedded by piezo layers is examined by Rafiee *et al*. (2014b). It is presumed that the CNTs are uniformly distributed and randomly oriented in the thin structure. Kamarian *et al*. (2018) calculate the natural frequency of MHC plates using the two dimensional GDQ scheme. In this paper Mori-Tanaka micromechanical rule is employed to extract the equivalent properties. Moreover, the firefly algorithm is introduced to determine the optimum stacking sequence of MHC plate. Axisymmetric vibration of MHC annular plate are inquired by Safarpour *et al*. (2020). In this work, higher order shear deformation plate theory is utilized to exploit the governing equations. Tornabene *et al*. (2019) evaluate the efficacy of homogenization models on the free vibration of multiscale hybrid composite conical shells. Applying the GDQ, Galerkin, and arc-length procedures, Gholami *et al*. (2018) present a numerical study on the nonlinear dynamic resonant of multiscale hybrid laminated plates. Dynamic instability studies of MHS cylindrical shells (Lee 2020), visco conical shells (Zarei *et al*. 2017 and Hajmohammad *et al*. 2018), spherical shells (Lee 2019, Lee and Hwang 2019) are accomplished in the literature. Dabbagh *et al*. (2020) conducted linear thermal buckling of three phase laminated composite beams utilizing the Galerkin method.

Despite numerous researches on the thermal and mechanical stability of structures made of different materials for instance linear and nonlinear thermal stability of functionally graded materials (Duc 2014, Kiani and Eslami 2010, Abdelhak *et al*. 2016), laminated composites (Chikh *et al*. 2017, Katariya *et al*. 2017, Safaei 2020), FG-CNT structures (Rafiee *et al*. 2013, Mohammadimehr and Alimirzaei 2017, Do *et al*. 2019, Duong *et al* 2020, Duc *et al*. 2019b), FG-GPLRC beams (Song *et al*. 2019, Wu *et al*. 2017, Kiani and Mirzaei 2018), and smart materials (Shahbazi *et al*. 2014, Shokravi 2018, Nguyen 2018, Talebizadehsardari *et al*. 2020b, Khorasani *et al*. 2020), according to the above literature review, nonlinear thermal stability response of MHC beams are not reported. Therefore, in order to fill the shortage of this phenomenon in the literature, this research deals with the thermal buckling and post-buckling of three phase CNT/fiber/matrix beams. The governing equations are extracted based on the first order shear deformation and Von-Karman geometrical nonlinearity theory. The generalized differential quadrature method are employed to transform the differential equations into the algebraic ones. The buckling temperature is determined using the obtained linear eigenvalue problem. Then, by exploiting the critical temperature and an iterative displacement marching technique, the displacement-load path are adopted. Multiscale hybrid composite homogenization follows a hierarchy. First, by means of Halpin-Tsai micromechanical rule, the effective material properties are obtained for a two phase CNT/matrix nanocomposite. Afterwards, the modified Chamis rule is implemented to capture the equivalent material

characteristics of CNT/fiber/matrix multiscale beam. After validation, the novel results show the repercussions of geometrical parameters, CNT and e-glass fiber agglomeration, number and model of layers variation on the thermal buckling and post-buckling of MHC beams.

2. Geometry and material properties multi-scale hybrid composite

A MHC beam with length L, thickness h is considered. This structure consists of N_L CNT/fiber/polymer ply. The beam is assumed under uniform temperature rise. It is supposed that each lamina of the multi-scale laminated composite beam is made of three phases; epoxy resin as matrix, isotropic carbon nanotubes, and E-glass fibers. CNTs are presumed to be uniformly and perfectly distributed and randomly oriented along the matrix. In addition, the directness, same thermo-mechanical properties and aspect ratio for CNTs are governed. CNT/Fiber/Matrix are perfectly bonded and there is no void (for its any types) in the matrix.

The equivalent thermo-mechanical properties are accounted in the two step hierarchy. Firstly, an isotropic nanocomposite is obtained using the Halpin-Tsai micromechanical rule with combining the CNTs and matrix (Dat *et al*. 2019). Then, by implementing the modified Chamis micromechanics approach, the fibers with different alignments for each lamina are applied into the two-phase nanocomposite.

The volume fraction of CNTs can be calculated by 6he following relation

$$V_{CN} = \frac{W_{CN}}{W_{CN} + \left(\frac{\rho_{CN}}{\rho_m}\right)(1 - W_{CN})} \tag{1}$$

where W_{CN} is the mass fraction of CNT and ρ_{CN} and ρ_m indicate the mass density of carbon nanotube and polymer, respectively. To take into account the geometry and size of nanotubes on the Young modulus, the Halpin-Tsai rule is propounded in the present work (Affdl and Kardos 1976). Based on this formula, the effective modulus of elasticity E_{MNC} for isotropic two-phase nanocomposite media can be written as

$$\begin{aligned} E_{MNC} = \frac{3}{8}\frac{1 + 2\left(\frac{\ell_{CN}}{d_{CN}}\right)\beta_{dl}V_{CN}}{1 - \beta_{dl}V_{CN}} \times E_m \\ + \frac{5}{8}\frac{1 + 2\beta_{dd}V_{CN}}{1 - \beta_{dd}V_{CN}} \times E_m \end{aligned} \tag{2}$$

It is worth nothing the thickness, diameter, and length of CNTs are demonstrated by t_{CN}, d_{CN}, and ℓ_{Cn}, respectively. β_{dl} and β_{dl} are two auxiliary factors that are expressed by

$$\beta_{dl} = \frac{\left(\frac{E_{CN}^{11}}{E_m}\right) - \left(\frac{d_{CN}}{4t_{CN}}\right)}{\left(\frac{E_{CN}^{11}}{E_m}\right) + \left(\frac{\ell_{CN}}{2t_{CN}}\right)}, \qquad \beta_{dl} = \frac{\left(\frac{E_{CN}^{11}}{E_m}\right) - \left(\frac{d_{CN}}{4t_{CN}}\right)}{\left(\frac{E_{CN}^{11}}{E_m}\right) + \left(\frac{d_{CN}}{2t_{CN}}\right)} \tag{3}$$

In the above equations E_m and E_{CN}^{11} are elastic constant of matrix and carbon nanotube, respectively. Therewith the Poisson's ratio, mass density and shear elastic constant are defined by

$$\begin{aligned} \nu_{MNC} &= \nu_m \\ \rho_{MNC} &= V_{CN}\rho_{CN} + V_m\rho_m \\ G_{MNC} &= \frac{E_{MNC}}{2(1 + \nu_{MNC})} \end{aligned} \tag{4}$$

With considering the state of randomly oriented CNTs, the thermal expansion coefficient of the matrix containing nanotubes can be calculated using the Schapery equation. This relation was proposed by Alamusi *et al*. (2013) which is appropriated for the nanocomposite media reinforced with randomly oriented short fibers such as carbon nanotubes.

$$\begin{aligned} \alpha_{MNC} = \frac{1}{2}\left\{\left(\frac{V_{CN}E_{CN}^{11}\alpha_{CN} + V_mE_m\alpha_m}{V_{CN}E_{CN}^{11} + V_mE_m}\right)(1 - \nu_{MNC})\right. \\ + \alpha_mV_m(1 + \nu_m) \\ \left. + \alpha_{CN}V_{CN}(1 + \nu_{CN})\right\} \end{aligned} \tag{5}$$

Here, α_{CN} and α_m are the thermal expansion factors of each constituent of CNT reinforced nanocomposite. In addition, V_m is the volume fraction of matrix and can be obtained using $V_m = 1 - V_{CN} - V_F$. The relations below can be used to reach the effective mechanical properties of CNT/fiber/polymer composite. These equations are proffered in an article by Chamis and Sendeckyj (1968) as follows

$$\begin{aligned} E_{11} &= V_FE_F^{11} + V_{MNC}E_{MNC} \\ \frac{1}{E_{22}} &= \frac{V_F}{E_F^{22}} + \frac{V_{MNC}}{E_{MNC}} \\ &\quad -V_FV_{MNC}\frac{\frac{\nu_F^2E_{MNC}}{E_F^{22}} + \frac{\nu_{MNC}^2E_F^{22}}{E_{MNC}} - 2\nu_F\nu_{MNC}}{V_FE_F^{22} + V_{MNC}E_{MNC}} \\ \frac{1}{G_{12}} &= \frac{V_F}{G_F^{12}} + \frac{V_{MNC}}{G_{MNC}} \\ \nu_{12} &= V_F\nu_F + V_{MNC}\nu_{MNC} \\ \rho &= V_F\rho_F + V_{MNC}\rho_{MNC} \end{aligned} \tag{1}$$

The subscript F and MNC illustrate the fiber and two-phase isotropic nanocomposite. E_{11} and E_{22} are the longitudinal and transverse elastic modulus, respectively and also G_{12} denotes the shear elastic modulus of multi-scale nanocomposite. The procedure to obtain thermal expansion of composite are shown in the following relation

$$\begin{aligned} \alpha_{11} &= \frac{V_FE_F^{11}\alpha_F^{11} + V_{MNC}E_{MNC}\alpha_{MNC}}{V_FE_F^{11} + V_{MNC}E_{MNC}} \\ \alpha_{22} &= (1 + \nu_F)V_F\alpha_F^{22} + (1 + \nu_{MNC})V_{MNC}\alpha_{MNC} \\ &\quad - \nu_{12}\alpha_{11} \end{aligned} \tag{7}$$

3. Theoretical formulations

Based on the first order shear deformation theory (FSDT) (Timoshenko theory), the displacements field (u, w) of an arbitrary assumed point in the composite media are exhibited in terms of the displacements and rotations of the middle surface

$$\begin{aligned} u(x,z) &= u_0(x) + z\psi(x) \\ w(x,z) &= w_0(x) \end{aligned} \tag{8}$$

In which u_0, w_0 are displacement of the reference plane $(z = 0)$ along x and z directions. Likewise, ψ indicates rotation of the beam cross section. Von-Karman type of geometrically nonlinear theory is widely utilized as strain-displacement relation, also used in this paper. This relation is indicated as follow (Reddy 2006, Karami *et al*. 2020, Cao *et al*. 2020)

$$\begin{aligned} \varepsilon_{xx} &= u_{0,x} + \frac{1}{2}w_{0,x}^2 + z\psi_{,x} \\ \gamma_{xz} &= \psi + w_{0,x} \end{aligned} \tag{9}$$

where ε_{xx} explains the inplane strain and γ_{xz} is out-of-plane strain or shear strain. The Hook law as a constitutive law deals with the linear thermo-elastic materials; for each ply of composite, they are written as

$$\begin{aligned} \sigma_{xx}^k &= \bar{Q}_{11}^k(\varepsilon_{xx} - \bar{\alpha}_{11}^k \Delta T) \\ \sigma_{xz}^k &= \bar{Q}_{55}^k \gamma_{xz} \end{aligned} \tag{10}$$

$\bar{Q}_{11}, \bar{Q}_{55}, \bar{\alpha}_{11}^k$ are the material constants of a layer with fibers-angle φ_k with respect to x-axes, where they are obtained using the follow equations (Reddy 2006)

$$\begin{aligned} \bar{Q}_{11}^k &= Q_{11}\cos^4\varphi_k + Q_{22}\sin^4\varphi_k \\ &\quad +2(Q_{12}+2Q_{66})\sin^2\varphi_k\cos^2\varphi_k \\ \bar{Q}_{55}^k &= Q_{55}\cos^2\varphi_k + Q_{44}\sin^2\varphi_k \\ \bar{\alpha}_{11}^k &= \alpha_{11}\cos^2\varphi_k + \alpha_{22}\sin^2\varphi_k \end{aligned} \tag{11}$$

In the above relations $Q_{ij}(i,j = 1,2,4,5,6)$ are known to be the reduced constants along the fiber direction and can be calculated using

$$\begin{aligned} Q_{11} &= \frac{E_{11}}{1-\nu_{12}\nu_{21}}, \quad Q_{22} = \frac{E_{22}}{1-\nu_{12}\nu_{21}} \\ Q_{12} &= \frac{E_{11}\nu_{21}}{1-\nu_{12}\nu_{21}}, \quad Q_{66} = G_{12} \\ Q_{44} &= G_{23}, \quad Q_{55} = G_{13} \end{aligned} \tag{12}$$

The stress resultants of beam considering the Timoshenko theory, which define the forces and moment of beam, are presented as (Ghanati and Safaei 2019)

$$\begin{aligned} N_{xx} &= \sum_{k=1}^{N_L}\int_{z_k}^{z_{k+1}} \sigma_{xx}^k dz \\ M_{xx} &= \sum_{k=1}^{N_L}\int_{z_k}^{z_{k+1}} z\sigma_{xx}^k dz \\ Q_{xz} &= \kappa\sum_{k=1}^{N_L}\int_{z_k}^{z_{k+1}} \sigma_{xz}^k dz \end{aligned} \tag{13}$$

N_{xx} is the membrane force, M_{xx} is the moment and Q_{xz} denotes the shear force. Furthermore, κ is the shear correction factor and its magnitude depends on the geometry, loads, and boundary condition, where the values of $\frac{5}{6}$ or $\frac{\pi^2}{12}$ are frequently used in different researches (Thanh *et al*. 2017, Nguyen *et al*. 2017). It is worth nothingthat, the former one is selected for the present study.

The equilibrium equations are obtained using the virtual deformation principle. In the absent of external exerted load, the total potential energy of composite beam is reduced to the virtual strain energy. This rule highlights that the extremum of system energy must be equal to zero.

$$\delta U = 0 \tag{14}$$

Here the δU is the virtual strain energy variation and may be expressed as

$$\delta U = \int_0^L \int_{-0.5h}^{+0.5h} (\sigma_{xx}\delta\varepsilon_{xx} + \kappa\sigma_{xz}\delta\varepsilon_{xz}) dz\, dx \tag{15}$$

Substituting the Eqs. (8)-(10) into Eq. (15) and employing the suitable mathematical simplifications, the equilibrium equations of a three phase composite beam are achieved in terms of stress resultants

$$\begin{aligned} \delta u_0&: \quad N_{xx,x} = 0 \\ \delta w_0&: \quad Q_{xz,x} + \left(N_{xx}w_{0,x}\right)_{,x} = 0 \\ \delta w_0&: \quad M_{xx,x} - Q_{xz} = 0 \end{aligned} \tag{16}$$

The governing equations of equilibrium can be written in terms of displacements by replacing the Eq. (13) in the above relations

$$A_{11}u_{0,xx} + A_{11}w_{0,xx}w_{0,x} + B_{11}\psi_{,xx} = 0 \tag{17}$$

$$A_{55}\psi_{,x} + A_{55}w_{0,xx} + N_{xx}w_{0,xx} = 0 \tag{18}$$

$$\begin{aligned} &B_{11}u_{0,xx} + B_{11}w_{0,xx}w_{0,x} + D_{11}\psi_{,xx} \\ &-A_{55}\psi - A_{55}w_{0,x} = 0 \end{aligned} \tag{19}$$

A_{11}, B_{11}, and $D_{11}$are the stretching, stretching-bending, and bending stiffness, respectively. Besides, A_{55} is the shear stiffness of beam which are calculated by

$$\begin{aligned} (A_{11}, B_{11}, D_{11}) &= \sum_{k=1}^{N_L}\int_{z_k}^{z_{k+1}} \bar{Q}_{11}^k(1, z, z^2)dz \\ A_{55} &= \sum_{k=1}^{N_L}\int_{z_k}^{z_{k+1}} \kappa\bar{Q}_{55}^k dz \end{aligned} \tag{20}$$

In this paper only clamped (C) boundary condition, which is suitable for thermal buckling and post-buckling of composite beams, is considered. The mathematical expression of this type of edge support can be written as

$$\text{for clamped edges (C)}: u_0 = \psi = w_0 = 0 \tag{21}$$

4. Pre-buckling analysis

In this part, the pre-buckling analysis is performed. Because of using bifurcation type of buckling, obtaining primary path is necessary. From the first equation of Eq. (16), we have

$$N^0_{xx,x} = 0 \;\rightarrow\; N^0_{xx} = \mathrm{C} \tag{22}$$

Where C, a constant, is attained using the integral from this relation and superscript 0 denotes the pre-buckling state. Since the beam is perfectly laterally undeformed before the buckling, the magnitudes of w and ψ are equal to zero. Also, considering the immovability of boundary conditions, the axial deformation is obtained as follow

$$u^{\,0}_{\,0} = 0 \tag{23}$$

Finally, the generated axial force may be calculated using the Eqs. (13)-(21)-(22) as follow

$$N^0_{xx} = -N^T \tag{24}$$

Where N^T can be compute exploiting the following relation

$$N^T = \sum_{k=1}^{N_L} \int_{z_k}^{z_{k+1}} Q^k_{11} \alpha^k_{11} \Delta T dz \tag{25}$$

ΔT represents the difference between the current temperature and the reference one.

5. Thermal buckling analysis

In this section, the adjacent equilibrium criterion is applied to establish the stability relations. Based on the previous section, we can derive the stability equations by considering a perturbation (displacement field with superscript 1) around the primary path as

$$\begin{aligned} u_0 &= u^0_0 + u^1_0 \\ w_0 &= w^0_0 + w^1_0 \\ \psi &= \psi^0 + \psi^1 \end{aligned} \tag{26}$$

Similar to displacements, the stress resultants can be defined with two branches

$$\begin{aligned} N_{xx} &= N^0_{xx} + N^1_{xx} \\ M_{xx} &= M^0_{xx} + M^1_{xx} \\ Q_{xz} &= Q^0_{xz} + Q^1_{xz} \end{aligned} \tag{27}$$

Now substituting the above equations in the equilibrium Eqs. (17)-(18)-(19), the terms in the obtained relations with superscript 0 satisfy the primary path and so are vanished from the equations. Moreover, because of their small values, the non-linear terms with superscript 1 are not considered. The captured terms after simplification take the forms below

$$A_{11} u^1_{0,xx} + B_{11} \psi^1_{,xx} = 0 \tag{28}$$

$$A_{55} \psi^1_{,x} + A_{55} w^1_{0,xx} - N^T w^1_{0,xx} = 0 \tag{29}$$

$$B_{11} u^1_{0,xx} + D_{11} \psi^1_{,xx} - A_{55} \psi^1 - A_{55} w^1_{0,x} = 0 \tag{30}$$

Implementing the described solution method in the next section, the above differential equations can be discreted in the composite beam domain into an eigenvalue system of algebraic.

$$\left(\mathbf{K_T} - N^T \mathbf{K_g}\right)\mathbf{U} = 0 \tag{31}$$

With solving the above problem, the critical axial force N^T is obtained conversely, the critical temperature can be computed utilizing Eq. (25).

6. Thermal post-buckling analysis

As mentioned below, the equilibrium equations in terms of displacement for the post-buckling analysis can be written as follow

$$A_{11} u_{0,xx} + A_{11} w_{0,xx} w_{0,x} + B_{11} \psi_{,xx} = 0 \tag{32}$$

$$\begin{aligned} &A_{55} \psi_{,x} + A_{55} w_{0,xx} \\ &+\left(A_{11} u_{0,x} + 0.5 A_{11} w^2_{0,x} + B_{11} \psi_{,x} - N^T\right) w_{0,xx} = 0 \end{aligned} \tag{33}$$

$$\begin{aligned} &B_{11} u_{0,xx} + B_{11} w_{0,xx} w_{0,x} \\ &+D_{11} \psi_{,xx} - A_{55} \psi - A_{55} w_{0,x} = 0 \end{aligned} \tag{34}$$

The super equations must be discreted and turn to algebraic equation using a numerical tool. For this process, in this paper the generalized differential quadrature method (GDQ) is employed as an effective numerical method. After specifying the system of nonlinear algebraic equations and considering the fact that the clamped supported is suitable for buckling and post-buckling, the compact form of equations takes the following form

$$\left(\mathbf{K_T}(\mathbf{U}) - N^T \mathbf{K_g}\right)\mathbf{U} = 0 \tag{35}$$

The obtained nonlinear eigenvalue problem is solved utilizing an iterative displacement control procedure. The target displacement is divided into the number of sub-displacement. This technique is the same with the one described in

(a) At first, by setting the zero magnitude for $\mathbf{U}$ in the elastic stiffness matrix, the buckling analysis is performed to account the critical temperature.
(b) Using the Eq. (35) related eigenvector with the calculated $\boldsymbol{T_{cr}}$ is specified.
(c) The determined eigenvector must be scaled-up according to the first step of target displacement.
(d) The established displacement is substituted in the elastic stiffness and then a new T_{cr} is obtained.
(e) Steps (b)-(d) must be repeated to reach a convergent value for T_{cr}.
(f) Next, the step of target displacement should be added and the above process needs to be repeated; finally, the target displacement and its related temperature are achieved.

7. GDQ method

The GDQ method was exploited to discrete the derivatives in the governed equilibrium equations and the associated boundary conditions. This technique allows to estimate any order derivative in an arbitrary point in the beam domain of a smooth function $\mathbf{u}$ employing a weighted linear sum of the function values at each delineated distributed points. For example, after applying the GDQ technique to the first and second order derivatives, the followings are obtained (Javani *et al*. 2019)

$$\begin{aligned}\mathbf{u}_{,x}|_{x=x_p} &= \sum_{p'=1}^{N_x} C_{pp'}^{x}\mathbf{u}|_{x=x_{p'}} \\ \mathbf{u}_{,xx}|_{x=x_p} &= \sum_{p'=1}^{N_x} \bar{C}_{pp'}^{x}\mathbf{u}|_{x=x_{p'}}, \quad p=1,2,\dots,N_x\end{aligned} \tag{36}$$

where N_x is the number of grid points in the x direction. Also, $C_{pp'}^{x}$ and $\bar{C}_{pp'}^{x}$ are the weighting coefficients of first and second order derivatives, respectively. These coefficients are determined using the Lagrange polynominal interpolation along the beam domain as

$$\begin{aligned}C_{pp'}^{x} &= \begin{cases}\dfrac{\Pi(x_p)}{(x_p-x_{p'})\Pi(x_{p'})} & \text{when} \quad p\neq p' \\ -\displaystyle\sum_{k=1,k\neq p}^{N_x} C_{pk}^{x} & \text{when} \quad p=p'\end{cases} \\ p,p' &= 1,2,\dots,N_\varphi\end{aligned} \tag{37}$$

in which

$$\Pi(x_p) = \prod_{k=1,k\neq p}^{N_x}(x_p-x_k), \tag{38}$$

and

$$\begin{cases}\bar{C}_{pp'}^{x} = 2\left(C_{pp}^{x}C_{pp'}^{x} - \dfrac{C_{pp'}^{x}}{(x_p-x_{p'})}\right), & p\neq p' \\ p,p' = 1,2,\dots,N_x \\ \bar{C}_{pp}^{x} = -\displaystyle\sum_{k=1,k\neq p}^{N_x}\bar{C}_{pk}^{x}, & p=p', \\ p = 1,2,\dots,N_x\end{cases} \tag{39}$$

It is worth mentioning that the Chebyshev-Gauss-Lobatto type of point distribution as an accurate types of grid dispensation is implemented in this essay. The location of each discrete point are obtained as

$$\begin{aligned}x_p &= L\left(\frac{1}{2}-\frac{1}{2}\cos\left(\frac{p-1}{N_x-1}\pi\right)\right), \\ p &= 1,2,\dots,N_x\end{aligned} \tag{40}$$

After applying this tool to the differential equations, a system of algebraic equations is obtained, where the solution method of these equations for thermal buckling and post-buckling are described in the previous sections.

Table 1 Thermomechanical properties of the three phase composite beam constituents GPLs (Chamis 1983, Rafiee *et al*. 2014a)

Properties	Magnitude	Unit
E_m	2.72	GPa
ρ_m	1200	kg/m ^{3}
ν_m	0.33	-
α_m	45×10^{-6}	1/K
E_{CN}	640	GPa
ρ_{CN}	1350	kg/m ^{3}
ν_{CN}	0.33	-
α_{CN}	3.4584×10^{-6}	1/K
$E_F^{11}=E_F^{22}$	73.0844	GPa
G_F^{12}	30.1301	GPa
ρ_F	2491.12	kg/m ^{3}
ν_F	0.22	-
$\alpha_F^{11}=\alpha_F^{22}$	1.5555×10^{-6}	1/K

8. Results and discussion

To investigate the thermal buckling and post-buckling of the mentioned composite beam, also to study the accuracy of the utilized methods, some numerical results are shown after validation. As mentioned before, in the current research E-glass fiber is selected as a macroscale phase, carbon nanotube as a nanoscale phase and finally epoxy resin polymer as a matrix. The material properties of each constituent of the three phase composite are demonstrated in Table 1. Furthermore, the geometry of used single walled nanotubes are as follow:

$$\ell_{CN} = 25\ \mu\text{m},\ d_{CN} = 1.4\ \text{nm},\ t_{CN} = 0.34\ \text{nm}.$$

Mass fraction of nanotubes W_{CN} and volume fraction of fiber reinforcement V_F will be illustrated for any specific result.

8.1 Convergence and comparison study

To assure the efficiency and accuracy of the applied methods, a few comparison studies should be performed Since there is not any research available on the thermal buckling/post-buckling of three phase composite beams, a comparison study is examined for an isotropic clamped beam. Fig. 1 compares the thermal buckling temperature with respect to the length-to-thickness ratio with the work by Eslami (2018). In the mentioned book, to obtain the critical temperature rise, an analytical solution is developed. A very good agreement is observed between the present results and that by Eslami (2018). Also, Fig. 2 represents the thermal post-buckling behavior of a clamped beam made of different isotropic materials. This study compares the obtained data by the suggested formulation and that presented by Eslami's book (Eslami 2018). A higher precision between these two works was noted. It is worth nothing that the material properties given in Table 2 is considered.

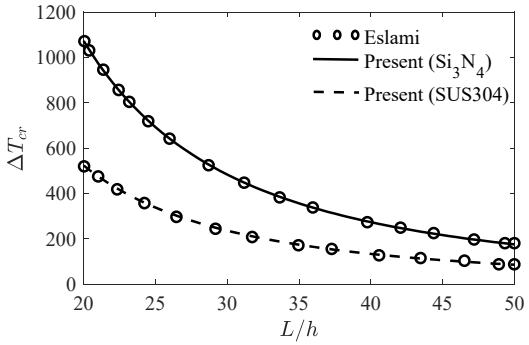

Fig. 1 Comparison of the thermal buckling temperature rise ΔT(K) with respect to the length-to-thickness ratio L/h for clamped beam made of two types of materials with the results of Eslami (2018)

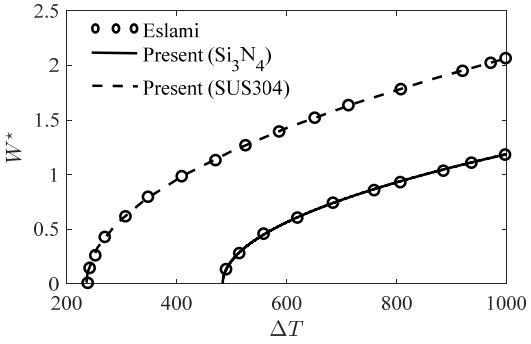

Fig. 2 Comparison temperature rise ΔT(K)-dimensionless deflection W^*(m/m) equilibrium paths path of homogeneous beams for two types of materials with Eslami (2018)

Table 2 Thermomechanical properties of SUS304 andSi_3N_4 (Eslami 2018)

Properties	Magnitude	Unit
E_{SUS304}	207.79	GPa
ν_{SUS304}	0.28	-
α_{SUS304}	15.3210×10^{-6}	1/K
$E_{Si_3N_4}$	322.27	GPa
$\nu_{Si_3N_4}$	0.28	-
$\alpha_{Si_3N_4}$	7.4746×10^{-6}	1/K

Table 3 Critical temperature change of $(0/90)_s$ three phase composite beams for different V_F, W_{CN}, and L/h

		V_F		
L/h	$W_{CN}(\%)$	0.6	0.7	0.8
60	0	353.556	429.268	507.031
	1	374.746	482.523	595.683
	2	329.138	435.811	554.213
	3	296.861	402.016	524.814
80	0	200.454	243.177	286.833
	1	211.819	272.613	336.293
	2	185.815	245.961	312.627
	3	167.484	226.759	295.915
100	0	128.763	156.147	184.059
	1	135.870	174.829	215.591
	2	119.122	157.658	200.344
	3	107.339	145.312	189.595

8.2 Parametric study

In this part, several parametric studies are propounded to investigate the thermal buckling and post-buckling of three phase composite beam. Table 3 gives information about the critical temperature change for various fiber volume fraction, mass fraction of CNTs and three magnitudes of length-to-thickness ratio. As mentioned in the previous section, the clamped boundary conditions are considered for beam edges. The orientation of fibers for each layer of laminated beam is (0/90/90/0). At first glance, it is manifest that fiber volume fraction decline makes a more stable structure and therefore thermal buckling temperature significantly improves. On the other hand, increasing the mass fraction of CNTs has two separate behavior. First, when the value of this number goes up from 0.0 to 1.0 percent, the critical temperature suddenly rises but after that with the growth of one makes a less stable structure; so critical temperature reduces. The reason of this treat is the large thermal expansion of nanotubes. Finally, as expected from the last result of this study, it can be concluded that the critical buckling temperature remarkably declines when the beam begins to become thinner.

In Fig. 3 the temperature-deflection equilibrium path of several types of three phase composite beam is examined. This figure includes four subfigures with various type of laminate. The directions of each layer of each laminate are highlighted in the figures. To develop the study, the volume fraction of fibers and mass fraction of nanotubes are assumed as $V_F = 0.6, W_{CN} = 3\%$. Each subfigure consists of the thermal post-buckling of three types of beam with $\frac{L}{h} = 60, 80, 100$. It can be observed the (0/45/45/0) is the most stable structure; whereas, the (0/30/60/90) is the least stable type of reinforcements. In this research, it can be seen from the last result of previous study that the higher L/h ratio results in the less stable structure.

Fig. 4 delineates the thermal post-postbuckling path of multiscale laminated beam for three magnitudes of fiber volume fraction. Each subfigure involves four values of the mass fraction of CNTs. The stacking sequence (0/90/90/0) with $\frac{L}{h} = 80$ is considered to examine this result. As indicated in the graphs, improving the amounts of the mass fraction of CNTs firstly causes a sharply boom; whereas; afterwards the increase of this amount due to the high thermal expansion makes a less stable structure for all values of V_F. It is worth mentioning that with an increase in the temperature, the structures that are reinforced by CNTs convert to more stable rather than the beams without any CNTs.

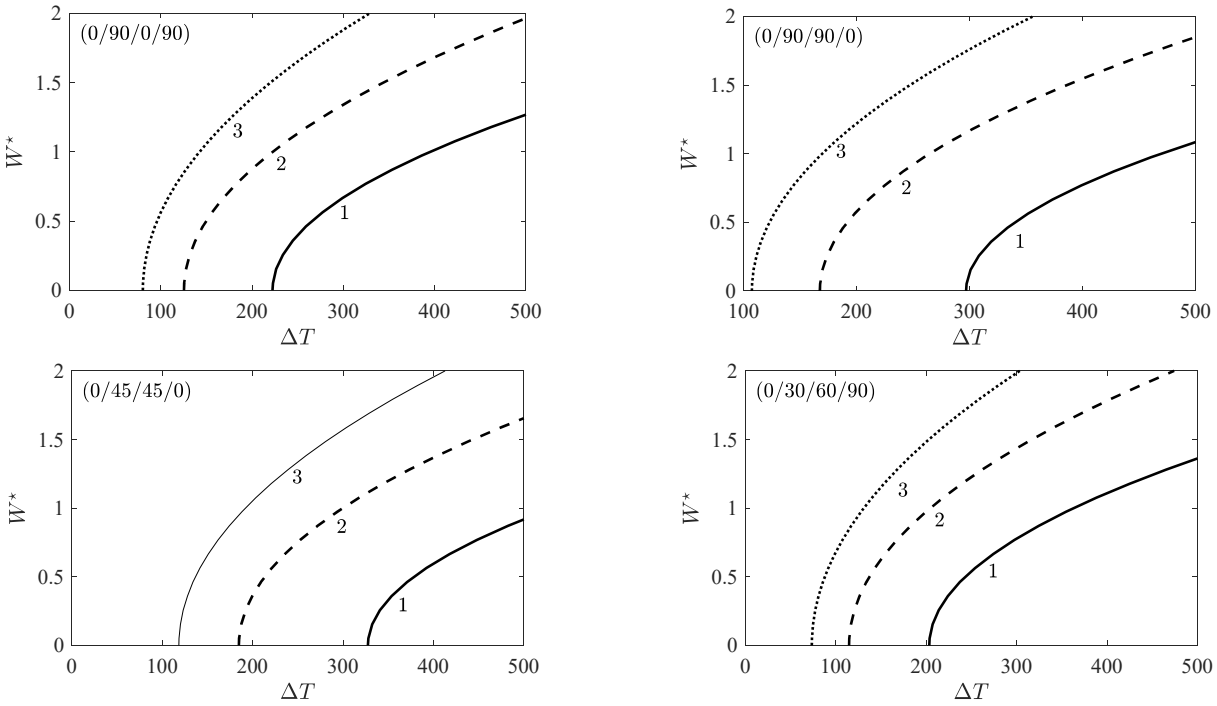

Fig. 3 Temperature rise ΔT(K)-dimensionless deflection W^*(m/m) equilibrium paths of clamped three phase beam for various layering model. (1: $L/h = 60$, 2: $L/h = 80$, 3: $L/h = 100$)

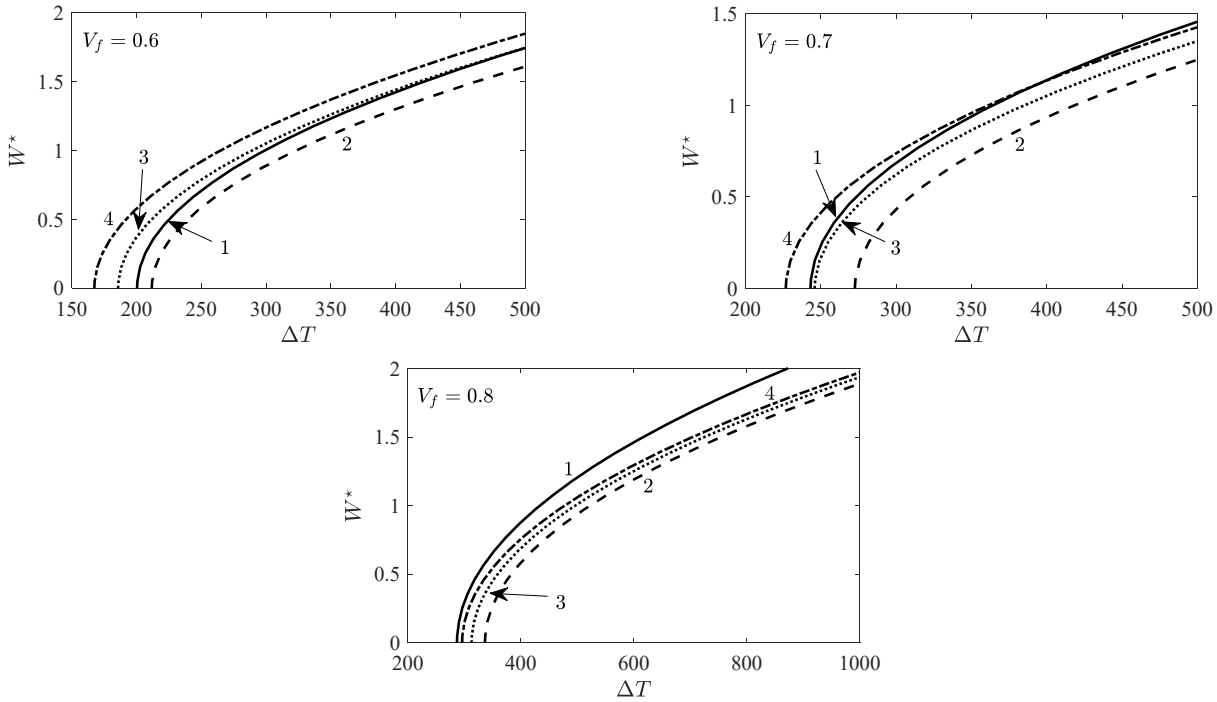

Fig. 4 Temperature rise ΔT(K)-dimensionless deflection W^*(m/m) equilibrium paths of clamped three phase beam for various fiber volume fraction. (1: $W_{CN} = 0\%$, 2: $W_{CN} = 1\%$, , 3: $W_{CN} = 2\%$, 4: $W_{CN} = 3\%$)

The specific amount of nanotubes that the buckling temperature and stability of the beam in the post-buckling path decrease after the increase depends on the composite layering. As viewed in the last result, with increasing the CNTs amount from 1.0 to 2.0 percent, the structure trends to become less stable, while in Fig. 5, which is modeled as (0/30/60/90), even with the nanotube increase by up to 3.0%, the buckling temperature and the stability of the structure grow; however, the slope of increasing plummets. It is noteworthy that the $V_F = 0.7$ and $\frac{L}{h} = 80$ are taken for the results in Fig. 5.

The effects of layer number on the post-buckling path are illustrated in Fig. 6. The volume fraction of fibers $V_F =$

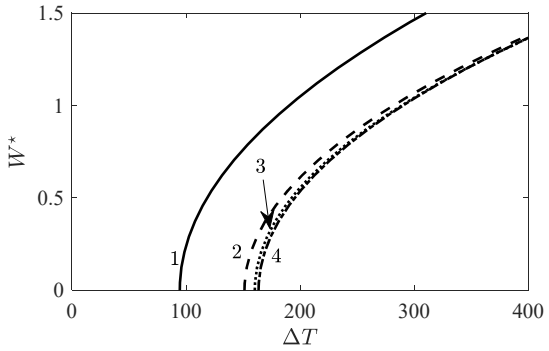

Fig. 5 Temperature rise ΔT(K)-dimensionless deflection W^*(m/m) equilibrium paths of (0/30/60/90) clamped three phase beam (1: $W_{CN} = 0\%$, 2: $W_{CN} = 1\%$, 3: $W_{CN} = 2\%$, 4: $W_{CN} = 3\%$)

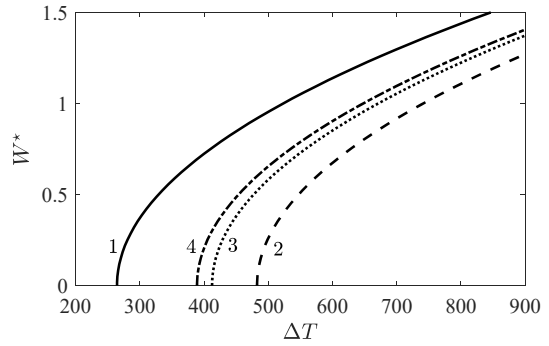

Fig. 6 Temperature rise ΔT(K)-dimensionless deflection W^*(m/m) equilibrium paths of clamped three phase beam. (1: (0/90) 2: $(0/90)_s$, 3: $(0/90)_{2s}$, 4: $(0/90)_{3s}$)

0.7, mass fraction of nanotubes $W_{CN} = 1\%$, and length-to-thickness ratio $\frac{L}{h} = 60$ are assumed. Four type of layering is presumed, that are denoted in the Fig. 6. According to the graph, with increasing the number of layer, the mid-plane deflection slumps (thermal buckling climbs), but then this amount slightly increases.

9. Conclusions

Based on the GDQ method and the iterative displacement control technique, the critical temperature rise and nonlinear equilibrium thermal path of MHC beams are calculated. The Halpin-Tsai and modified Chamis homogenization legislations are implemented to model the mentioned three phase composite structure. The first order shear deformation, nonlinear strain-displacement relations, linear thermoelastic constitutive law, and finally virtual work principle are utilized to extract the governing equilibrium equations on the thermoelastic response of laminated beam. Effects of geometrical factors and layering types and furthermore the advantage of adding CNT and fibers into the composite are analyzed by some numerical outcomes. In can be concluded that:

- Congestion of fibers always increases the buckling temperature; however, addition of CNTs firstly enhances the critical temperature due to its high stiffness but then with increasing the CNT weight fraction, the buckling temperature is decreased because the effect of its thermal expansion overcomes that of its elasticity modulus.
- The magnitude of CNTs that the slope of temperature buckling increase is varied to negative significantly depends on the layering procedure and fibers orientation.
- Enlarging the length-to-thickness ratio dramatically deteriorates the structure stiffness.
- The MHC beams behaves differently for various number of plies and also layering models; depending on the direction of fibers toward the beam length, the structure experiences more rigid.

Acknowledgments

This research is financially supported by the Ministry of Science and Technology of China (Grant No. 2019YFE0112400, 2018YFC1504303), the Key Research and Development Program of Liaoning Province (Grant No. 2017231010), the Taishan Scholar Priority Discipline Talent Group program funded by the Shandong Province, and the first-class discipline project funded by the Education Department of Shandong Province.

References

Abdelhak, Z., Hadji, L., Daouadji, T.H. and Adda Bedia, E.A. (2016), "Thermal buckling response of functionally graded sandwich plates with clamped boundary conditions", *Smart Struct. Syst., Int. J.*, **18**(2), 267-291. https://doi.org/10.12989/sss.2016.18.2.267

Affdl, J.H. and Kardos, J.L. (1976), "The Halpin-Tsai equations: a review", *Polym. Eng. Sci.*, **16**(5), 344-352 https://doi.org/10.1002/pen.760160512

Alamusi, A., Hu, N., Qiu, J., Li, Y., Chang, C., Atobe, S., Fukunaga, H., Liu, Y., Ning, H., Wu, L. and Li, J. (2013), "Multi-scale numerical simulations of thermal expansion properties of CNT-reinforced nanocomposites", *Nanoscale Res. Lett.*, **8**(1), 15-15. https://doi.org/10.1186/1556-276X-8-15

Bekyarova, E., Thostenson, E.T., Yu, A., Kim, H., Gao, J., Tang, J., Hahn, H.T., Chou, T.W., Itkis, M.E. and Haddon, R.C. (2007a), "Multiscale carbon nanotube− carbon fiber reinforcement for advanced epoxy composites", *Langmuir*, **23**(7), 3970-3974. https://doi.org/10.1021/la062743p

Bekyarova, E., Thostenson, E.T., Yu, A., Itkis, M.E., Fakhrutdinov, D., Chou, T.W. and Haddon, R.C. (2007b), "Functionalized single-walled carbon nanotubes for carbon fiber−epoxy composites", *J. Phys. Chem. C*, **111**(48), 17865-17871. https://doi.org/10.1021/jp071329a

Cao, Y., Musharavati, F., Baharom, S., Talebizadehsardari, P., Sebaey, T.A., Eyvazian, A. and Zain, A.M. (2020), "Vibration response of FG-CNT-reinforced plates covered by magnetic layer utilizing numerical solution", *Steel Compos. Struct., Int. J.*, **37**(2), 253-258. https://doi.org/10.12989/scs.2020.37.2.253

Chamis, C.C. (1983), "Simplified composite micromechanics equations for hygral, thermal and mechanical properties".

Chamis, C.C. and Sendeckyj, G.P. (1968), "Critique on theories

predicting thermoelastic properties of fibrous composites", *J. Compos. Mater.*, **2**(3), 332-358. https://doi.org/10.1177/002199836800200305

Chikh, A., Tounsi, A., Hebali, H. and Mahmoud, S.R. (2017), "Thermal buckling analysis of cross-ply laminated plates using a simplified HSDT", *Smart Struct. Syst.*, *Int. J.*, **19**(3), 289-297. https://doi.org/10.12989/sss.2017.19.3.289

Dabbagh, A., Rastgoo, A. and Ebrahimi, F. (2020), "Thermal buckling analysis of agglomerated multiscale hybrid nanocomposites via a refined beam theory", *Mech. Based. Des. Struc.*, pp. 1-27. https://doi.org/10.1080/15397734.2019.1692666

Dat, N.D., Quan, T.Q. and Duc, N.D. (2019), "Nonlinear thermal vibration of carbon nanotube polymer composite elliptical cylindrical shells", *Int. J. Mech. Mater. Des.*, 1-20. https://doi.org/ 10.1007/s10999-019-09464-y

Dat, N.D., Quan, T.Q., Mahesh, V. and Duc, N.D. (2020a), "Analytical solutions for nonlinear magneto-electro-elastic vibration of smart sandwich plate with carbon nanotube reinforced nanocomposite core in hygrothermal environment", *Int. J. Mech. Sci.*, **186**, p. 105906. https://doi.org/10.1016/j.ijmecsci.2020.105906

Dat, N.D., Khoa, N.D., Nguyen, P.D. and Duc, N.D. (2020b), "An analytical solution for nonlinear dynamic response and vibration of FG-CNT reinforced nanocomposite elliptical cylindrical shells resting on elastic foundations", *ZAMM-Z ANGEW MATH ME*, **100**(1), p. e201800238. https://dx.doi.org/10.1002/zamm.201800238

Do, Q.C., Pham, D.N., Vu, D.Q., Vu, T.T.A. and Nguyen, D.D. (2019), "Nonlinear buckling and post-buckling of functionally graded CNTs reinforced composite truncated conical shells subjected to axial load", *Steel Compos. Struct.*, *Int. J.*, **31**(3), 243-259. http://dx.doi.org/10.12989/scs.2019.31.3.243

Duc, N.D. (2014), "Nonlinear static and dynamic stability of functionally graded plates and shells", Vietnam National University Press, Hanoi, Vietnam.

Duc, N.D., Hadavinia, H., Quan, T.Q. and Khoa, N.D. (2019a), "Free vibration and nonlinear dynamic response of imperfect nanocomposite FG-CNTRC double curved shallow shells in thermal environment", *Eur. J. Mech. A Solids.*, **75**, 355-366. https://doi.org/10.1016/j.euromechsol.2019.01.024

Duc, N.D., Nguyen, P.D., Cuong, N.H., Van Sy, N. and Khoa, N.D. (2019b), "An analytical approach on nonlinear mechanical and thermal post-buckling of nanocomposite double-curved shallow shells reinforced by carbon nanotubes", *Proc. Inst. Mech. Eng., Part C*, **233**(11), 3888-3903. https://doi.org/10.1177/0954406218802921

Duong, T.M., Vu, T.T.A., Pham, D.N. and Nguyen, D.D. (2020), "Nonlinear post-buckling of CNTs reinforced sandwich-structured composite annular spherical shells", *Int. J. Struct. Stab. Dyn.*, **20**(2). https://dx.doi.org/10.1142/S0219455420500182

Ebrahimi, F. and Dabbagh, A. (2019), "On thermo-mechanical vibration analysis of multi-scale hybrid composite beams", *J. Vib. Control*, **25**(4), 933-945. https://doi.org/10.1177/1077546318806800

Eslami, M.R. (2018), "Buckling and Postbuckling of Beams, Plates, and Shells". Cham, Switzerland: Springer International Publishing.

Eyvazian, A., Musharavati, F., Tarlochan, F., Pasharavesh, A., Rajak, D.K., Husain, M.B. and Tran, T.N. (2020a), "Free vibration of FG-GPLRC conical panel on elastic foundation", *Struct. Eng. Mech., Int. J.*, **75**(1), 1-18. https://doi.org/10.12989/sem.2020.75.1.001

Eyvazian, A., Musharavati, F., Talebizadehsardari, P. and Sebaey, T.A. (2020b), "Free vibration of FG-GPLRC spherical shell on two parameter elastic foundation", *Steel Compos. Struct., Int. J.*, **36**(6), 711-727. https://doi.org/10.12989/scs.2020.36.6.711

Eyvazian, A., Shahsavari, D. and Karami, B. (2020c), "On the dynamic of graphene reinforced nanocomposite cylindrical shells subjected to a moving harmonic load", *Int. J. Eng. Sci.*, **154**, p.103339. https://doi.org/10.1016/j.ijengsci.2020.103339

Fattahi, A.M., Safaei, B. and Ahmed, N.A. (2019a), "A comparison for the non-classical plate model based on axial buckling of single-layered graphene sheets", *Eur. Phys. J. Plus.*, **134**(11), p. 555. https://doi.org/10.1140/epjp/i2019-12912-7

Fattahi, A.M., Safaei, B. and Moaddab, E. (2019b), "The application of nonlocal elasticity to determine vibrational behavior of FG nanoplates", *Steel Compos. Struct., Int. J.*, **32**(2), 281-292. https://doi.org/10.12989/scs.2019.32.2.281

Ghanati, P. and Safaei, B. (2019), "Elastic buckling analysis of polygonal thin sheets under compression", *Indian J. Phys.*, **93**(1), 47-52. https://doi.org/10.1007/s12648-018-1254-9

Ghasemi, A.R., Mohammadi, M.M. and Mohandes, M. (2015), "The role of carbon nanofibers on thermo-mechanical properties of polymer matrix composites and their effect on reduction of residual stresses", *Compos. B. Eng.*, **77**, 519-527. https://doi.org/10.1016/j.compositesb.2015.03.065

Ghasemi, A.R., Mohammadi Fesharaki, M. and Mohandes, M. (2017), "Three-phase micromechanical analysis of residual stresses in reinforced fiber by carbon nanotubes", *J. Compos. Mater.*, **51**(12), 1783-1794. https://doi.org/10.1177/0021998316669854

Gholami, R. and Ansari, R. (2018), "Nonlinear bending of third-order shear deformable carbon nanotube/fiber/polymer multiscale laminated composite rectangular plates with different edge supports", *Eur. Phys. J. Plus*, **133**(7), 282. https://doi.org/10.1140/epjp/i2018-12103-2

Gholami, R., Ansari, R. and Gholami, Y. (2018), "Numerical study on the nonlinear resonant dynamics of carbon nanotube/fiber/polymer multiscale laminated composite rectangular plates with various boundary conditions", *Aerosp. Sci. Technol.*, **78**, 118-129. https://doi.org/10.1016/j.ast.2018.03.043

Hajmohammad, M.H., Azizkhani, M.B. and Kolahchi, R. (2018), "Multiphase nanocomposite viscoelastic laminated conical shells subjected to magneto-hygrothermal loads: Dynamic buckling analysis", *Int. J. Mech. Sci.*, **137**, 205-213. https://doi.org/10.1016/j.ijmecsci.2018.01.026

Han, S., Meng, Q., Araby, S., Liu, T. and Demiral, M. (2019), "Mechanical and electrical properties of graphene and carbon nanotube reinforced epoxy adhesives: experimental and numerical analysis", *Compos. Part A. Appl.*, **120**, 116-126. https://doi.org/10.1016/j.compositesa.2019.02.027

He, X.Q., Rafiee, M., Mareishi, S. and Liew, K.M. (2015), "Large amplitude vibration of fractionally damped viscoelastic CNTs/fiber/polymer multiscale composite beams", *Compos. Struct.*, **131**, 1111-1123. https://doi.org/10.1016/j.compstruct.2015.06.038

Javani, M., Kiani, Y. and Eslami, M.R. (2019), "Geometrically nonlinear rapid surface heating of temperature-dependent FGM arches", *Aerosp. Sci. Technol.*, **90**, 264-274. https://doi.org/10.1016/j.ast.2019.04.049

Kamarian, S., Shakeri, M. and Yas, M.H. (2018), "Natural frequency analysis and optimal design of CNT/fiber/polymer hybrid composites plates using mori-tanaka approach, GDQ technique, and firefly algorithm", *Polym. Compos.*, **39**(5), 1433-1446. https://doi.org/10.1002/pc.24083

Karami, B., Shahsavari, D., Ordookhani, A., Gheisari, P., Li, L. and Eyvazian, A. (2020), "Dynamics of graphene-nanoplatelets reinforced composite nanoplates including different boundary conditions", *Steel Compos. Struct., Int. J.*, **36**(6), 689-702. https://doi.org/10.12989/scs.2020.36.6.689

Katariya, P., Panda, S.K., Hirwani, C.K., Mehar, K. and Thakare, O. (2017), "Enhancement of thermal buckling strength of

laminated sandwich composite panel structure embedded with shape memory alloy fibre", *Smart Struct. Syst.*, *Int. J.*, **20**(5), 595-605. https://doi.org/10.12989/sss.2017.20.5.595

Khorasani, M., Eyvazian, A., Karbon, M., Tounsi, A., Lampani, L. and Sebaey, T.A. (2020), "Magneto-electro-elastic vibration analysis of modified couple stress-based three-layered micro rectangular plates exposed to multi-physical fields considering the flexoelectricity effects", *Smart Struct. Syst.*, *Int. J.*, **26**(3), 331-343. https://doi.org/10.12989/sss.2020.26.3.331

Kiani, Y. and Eslami, M.R. (2010), Thermal buckling analysis of functionally graded material beams", *Int. J. Mech. Mater. Des.*, **6**(3), 229-238. https://doi.org/10.1007/s10999-010-9132-4

Kiani, Y. and Mirzaei, M. (2018), "Enhancement of non-linear thermal stability of temperature dependent laminated beams with graphene reinforcements", *Compos. Struct.*, **186**, 114-122. https://doi.org/10.1016/j.compstruct.2017.11.086

Kim, M., Park, Y.B., Okoli, O.I. and Zhang, C. (2009), "Processing, characterization, and modeling of carbon nanotube-reinforced multiscale composites", *Compos. Sci. Technol.*, **69**(3-4), 335-342. https://doi.org/10.1016/j.compscitech.2008.10.019

Lee, S.Y. (2019), "Dynamic instability of carbon nanotubes/fiber/polymer multiscale composite spherical shells with delamination around a cutout", *Int. J. Struct. Stab. Dy.*, **19**(11), 1950132. https://doi.org/10.1142/S0219455419501323

Lee, S.Y. (2020), "Dynamic stability and nonlinear transient behaviors of CNT-reinforced fiber/polymer composite cylindrical panels with delamination around a cutout", *Nonlinear Dyn.*, 1-19. https://doi.org/10.1007/s11071-020-05477-x.

Lee, S.Y. and Hwang, J.G. (2019), "Finite element nonlinear transient modelling of carbon nanotubes reinforced fiber/polymer composite spherical shells with a cutout", *Nanotechnol. Rev.*, **8**(1), 444-451. https://doi.org/10.1515/ntrev-2019-0039

Mohammadimehr, M. and Alimirzaei, S. (2017), "Buckling and free vibration analysis of tapered FG-CNTRC micro Reddy beam under longitudinal magnetic field using FEM", *Smart Struct. Syst.*, *Int. J.*, **19**(3), 309-322. https://doi.org/10.12989/sss.2017.19.3.309

Motezaker, M. and Eyvazian, A. (2020), "Buckling load optimization of beam reinforced by nanoparticles", *Struct. Eng. Mech.*, *Int. J.*, **73**(5), 481-486. https://doi.org/10.12989/sem.2020.73.5.481

Nguyen, D.D. (2018), "Nonlinear thermo-electro-mechanical dynamic response of shear deformable piezoelectric sigmoid functionally graded sandwich circular cylindrical shells on elastic foundations", *J. Sandw. Struct. Mater.*, **20**(3), 351-378. https://doi.org/10.1177/1099636216653266

Nguyen, D.D. and Pham, D.N. (2017), "The dynamic response and vibration of functionally graded carbon nanotubes reinforced composite (FG-CNTRC) truncated conical shells resting on elastic foundation", *Materials*, **10**(10), p. 1194. https://doi.org/10.3390/ma10101194

Nguyen, D.D., Tran, Q.Q. and Nguyen, D.K. (2017), "New approach to investigate nonlinear dynamic response and vibration of imperfect functionally graded carbon nanotube reinforced composite double curved shallow shells subjected to blast load and temperature", *Aerosp. Sci. Technol.*, **71**, 360-372. https://doi.org/10.1016/j.ast.2017.09.031

Radue, M.S. and Odegard, G.M. (2018), "Multiscale modeling of carbon fiber/carbon nanotube/epoxy hybrid composites: Comparison of epoxy matrices", *Compos. Sci. Technol.*, **166**, 20-26. https://doi.org/10.1016/j.compscitech.2018.03.006.

Rafiee, M., Yang, J. and Kitipornchai, S. (2013), "Thermal bifurcation buckling of piezoelectric carbon nanotube reinforced composite beams", *Comput. Math. Appl.*, **66**(7), 1147-1160. https://doi.org/10.1016/j.camwa.2013.04.031

Rafiee, M., He, X.Q., Mareishi, S. and Liew, K.M. (2014a), "Modeling and stress analysis of smart CNTs/fiber/polymer multiscale composite plates", *Int. J. Appl. Mech.*, **6**(3), 1450025. https://doi.org/10.1142/S1758825114500252

Rafiee, M., Liu, X.F., He, X.Q. and Kitipornchai, S. (2014b), "Geometrically nonlinear free vibration of shear deformable piezoelectric carbon nanotube/fiber/polymer multiscale laminated composite plates", *J. Sound Vib.*, **333**(14), 3236-3251. https://doi.org/10.1016/j.jsv.2014.02.033

Rafiee, M., Nitzsche, F. and Labrosse, M.R. (2018), "Cross-sectional design and analysis of multiscale carbon nanotubes-reinforced composite beams and blades", *Int. J. Appl. Mech.*, **10**(3), 1850032. https://doi.org/10.1142/S1758825118500321

Rahman, M.M., Zainuddin, S., Hosur, M.V., Malone, J.E., Salam, M.B.A., Kumar, A. and Jeelani, S. (2012), "Improvements in mechanical and thermo-mechanical properties of e-glass/epoxy composites using amino functionalized MWCNTs", *Compos. Struct.*, **94**(8), 2397-2406. https://doi.org/10.1016/j.compstruct.2012.03.014

Rahmanian, S., Suraya, A.R., Shazed, M.A., Zahari, R. and Zainudin, E.S. (2014), "Mechanical characterization of epoxy composite with multiscale reinforcements: carbon nanotubes and short carbon fibers", *Mater. Des.*, **60**, 34-40. https://doi.org/10.1016/j.matdes.2014.03.039

Reddy, J.N. (2006), *Theory and Analysis of Elastic Plates and Shells*, CRC press.

Rodriguez, A.J., Guzman, M.E., Lim, C.S. and Minaie, B. (2011), "Mechanical properties of carbon nanofiber/fiber-reinforced hierarchical polymer composites manufactured with multiscale-reinforcement fabrics", *Carbon*, **49**(3), 937-948. https://doi.org/10.1016/j.carbon.2010.10.057

Safarpour, M., Rahimi, A., NoormohammadiArani, O. and Rabczuk, T. (2020), "Frequency characteristics of multiscale hybrid nanocomposite annular plate based on a Halpin–Tsai homogenization model with the aid of GDQM", *Appl. Sci.*, **10**(4), 1412. https://doi.org/10.3390/app10041412

Safaei, B. (2020), "The effect of embedding a porous core on the free vibration behavior of laminated composite plates", *Steel Compos. Struct.*, *Int. J.*, **35**(5), 659-670. https://doi.org/10.12989/SCS.2020.35.5.659

Safaei, B., Khoda, F.H. and Fattahi, A.M. (2019), "Non-classical plate model for single-layered graphene sheet for axial buckling", *Adv. Nano Res.*, *Int. J.*, **7**(4), 265-277. https://doi.org/10.12989/anr.2019.7.4.265

Seidi, J. and Kamarian, S. (2017), "Free vibrations of non-uniform CNT/fiber/polymer nanocomposite beams", *Curved Layer. Struct.*, **4**(1), 21-30. https://doi.org/10.1515/cls-2017-0003

Shahbazi, Y., Delavari, E. and Chenaghlou, M.R. (2014), "Predicting the buckling load of smart multilayer columns using soft computing tools", *Smart Struct. Syst.*, *Int. J.*, **13**(1), 81-98. https://doi.org/10.12989/sss.2014.13.1.081

Shokravi, M. (2018), "Dynamic buckling of smart sandwich beam subjected to electric field based on hyperbolic piezoelasticity theory", *Smart Struct. Syst.*, *Int. J.*, **22**(3), 327-334. https://doi.org/10.12989/sss.2018.22.3.327

Shokrieh, M.M., Daneshvar, A., Akbari, S. and Chitsazzadeh, M. (2013), "The use of carbon nanofibers for thermal residual stress reduction in carbon fiber/epoxy laminated composites", *Carbon*, **59**, 255-263. https://doi.org/10.1016/j.carbon.2013.03.016

Song, Y.S. (2007), "Multiscale fiber-reinforced composites prepared by vacuum-assisted resin transfer molding", *Polym. Compos.*, **28**(4), 458-461. https://doi.org/10.1002/pc.20301

Song, M., Chen, L., Yang, J., Zhu, W. and Kitipornchai, S. (2019), "Thermal buckling and postbuckling of edge-cracked functionally graded multilayer graphene nanocomposite beams

on an elastic foundation", *Int. J. Mech. Sci.*, **161**, 105040. https://doi.org/10.1016/j.ijmecsci.2019.105040

Sung, D.H., Kim, M. and Park, Y.B. (2018), "Prediction of thermal conductivities of carbon-containing fiber-reinforced and multiscale hybrid composites", *Compos. Part B Eng.*, **133**, 232-239. https://doi.org/10.1016/j.compositesb.2017.09.032

Talebizadehsardari, P., Eyvazian, A., Musharavati, F., Mahani, R.B. and Sebaey, T.A. (2020a), "Elastic Wave Characteristics of Graphene Reinforced Polymer Nanocomposite Curved Beams Including Thickness Stretching Effect", *Polymers*, **12**(10), p. 2194. https://doi.org/10.3390/polym12102194

Talebizadehsardari, P., Eyvazian, A., Azandariani, M.G., Tran, T.N., Rajak, D.K. and Mahani, R.B. (2020b), "Buckling analysis of smart beams based on higher order shear deformation theory and numerical method", *Steel Compos. Struct., Int. J.*, **35**(5), 635-640. https://doi.org/10.12989/scs.2020.35.5.635

Thanh, N.V., Khoa, N.D., Tuan, N.D., Tran, P. and Duc, N.D. (2017), "Nonlinear dynamic response and vibration of functionally graded carbon nanotube-reinforced composite (FG-CNTRC) shear deformable plates with temperature-dependent material properties and surrounded on elastic foundations", *J. Therm. Stress.*, **40**(10), 1254-1274. https://doi.org/10.1080/01495739.2017.1338928

Thostenson, E.T., Li, W.Z., Wang, D.Z., Ren, Z.F. and Chou, T.W. (2002), "Carbon nanotube/carbon fiber hybrid multiscale composites", *J. Appl. Phys.*, **91**(9), 6034-6037. https://doi.org/10.1063/1.1466880.

Tornabene, F., Bacciocchi, M., Fantuzzi, N. and Reddy, J.N. (2019), "Multiscale approach for three-phase CNT/polymer/fiber laminated nanocomposite structures", *Polym. Compos.*, **40**(S1), E102-E126. https://doi.org/10.1002/pc.24520

Van Thanh, N., Dinh Quang, V., Dinh Khoa, N., Seung-Eock, K. and Dinh Duc, N. (2019), "Nonlinear dynamic response and vibration of FG CNTRC shear deformable circular cylindrical shell with temperature-dependent material properties and surrounded on elastic foundations", *J. Sandw. Struct. Mater*, **21**(7), 2456-2483. https://doi.org/10.1177/1099636217752243

Wu, H., Kitipornchai, S. and Yang, J. (2017), "Thermal buckling and postbuckling of functionally graded graphene nanocomposite plates", *Mater. Des.*, **132**, 430-441. https://doi.org/10.1016/j.matdes.2017.07.025

Zarei, M.S., Azizkhani, M.B., Hajmohammad, M.H. and Kolahchi, R. (2017), "Dynamic buckling of polymer–carbon nanotube–fiber multiphase nanocomposite viscoelastic laminated conical shells in hygrothermal environments", *J. Sandw. Struct. Mater.*, 1099636217743288. https://doi.org/10.1177/1099636217743288

CC